

special communication

A modular NIRS system for clinical measurement of impaired skeletal muscle oxygenation

RAMESH WARIAR,^{1,3} JOHN N. GAFFKE,^{1,3}
RONALD G. HALLER,^{1,2,4} AND LOREN A. BERTOCCI^{1,5}

¹Institute for Exercise and Environmental Medicine, Presbyterian Hospital of Dallas, Dallas 75231;

²Department of Veterans Affairs Medical Center and Departments of ³Biomedical Engineering,

⁴Neurology, and ⁵Radiology, University of Texas Southwestern Medical Center, Dallas, Texas 75235

Wariar, Ramesh, John N. Gaffke, Ronald G. Haller, and Loren A. Bertocci. A modular NIRS system for clinical measurement of impaired skeletal muscle oxygenation. *J. Appl. Physiol.* 88: 315–325, 2000.—Near-infrared spectrometry (NIRS) is a well-known method used to measure in vivo tissue oxygenation and hemodynamics. This method is used to derive relative measures of hemoglobin (Hb) + myoglobin (Mb) oxygenation and total Hb (tHb) accumulation from measurements of optical attenuation at discrete wavelengths. We present the design and validation of a new NIRS oxygenation analyzer for the measurement of muscle oxygenation kinetics. This design optimizes optical sensitivity and detector wavelength flexibility while minimizing component and construction costs. Using in vitro validations, we demonstrate 1) general optical linearity, 2) system stability, and 3) measurement accuracy for isolated Hb. Using in vivo validations, we demonstrate 1) expected oxygenation changes during ischemia and reactive hyperemia, 2) expected oxygenation changes during muscle exercise, 3) a close correlation between changes in oxyhemoglobin and oxymyoglobin and changes in deoxyhemoglobin and deoxymyoglobin and limb volume by venous occlusion plethysmography, and 4) a minimal contribution from movement artifact on the detected signals. We also demonstrate the ability of this system to detect abnormal patterns of tissue oxygenation in a well-characterized patient with a deficiency of skeletal muscle coenzyme Q₁₀. We conclude that this is a valid system design for the precise, accurate, and sensitive detection of changes in bulk skeletal muscle oxygenation, can be constructed economically, and can be used diagnostically in patients with disorders of skeletal muscle energy metabolism.

near-infrared spectrometry; hemoglobin; myoglobin; exercise; movement artifacts; metabolic disease; coenzyme Q₁₀ deficiency

NEAR-INFRARED SPECTROMETRY (NIRS) is a well-established technique for monitoring hemoglobin (Hb) and

The costs of publication of this article were defrayed in part by the payment of page charges. The article must therefore be hereby marked "advertisement" in accordance with 18 U.S.C. Section 1734 solely to indicate this fact.

myoglobin (Mb) oxygenation in vivo and noninvasively at the site of tissue (8, 9, 12). Briefly, with this method, optical absorption is measured across tissue (such as the forearm or head) at multiple wavelengths. Relative estimates of changes in oxygenation are calculated from the wavelength-specific absorption and the specific extinction coefficients of Hb and Mb (also known in the literature as the NIRS "algorithm") (29). As valuable as these sorts of measurements may be, there are very few available, much less affordable, NIRS devices (Table 1). Although a few can be purchased commercially (7, 9, 17, 26), others are available only if constructed on the basis of their descriptions in the literature (10, 11). In general, commercially available instruments are very simple in construction (e.g., Run-Man, NIM), at the possible expense of signal-to-noise ratio and optical sensitivity, or are very complex in construction [e.g., NIRO 500 (Hamamatsu, Bridgewater, NJ) or Oximeter (ISS)] and expensive (Table 1).

None of the available instruments, either those described in the literature or those that are commercially available, are designed in a modular fashion or to allow for changes to be made in wavelengths at which measurements are made. Therefore, we present the design of a new NIRS system that addresses all these design limitations. Although the described NIRS system is based on methodology previously reported (7, 9, 24, 29), the principal advantages of the design presented here are that 1) it is based on a broadband light source in combination with continuous light measurement (i.e., without light intensity modulation), 2) it is modular (i.e., it provides the flexibility to vary the wavelengths at which measurements are made), 3) it is simple, 4) it is easy to build, and 5) because it relies on readily available and relatively inexpensive optoelectronic components, any analog-to-digital converter, and any desktop personal computer, it is inexpensive to build.

Using a combination of in vitro and in vivo measurements, we demonstrate that 1) this design produces a stable and optically linear instrument, 2) it can detect

Table 1. Selection of available NIRS devices

Device	Approximate Cost, \$	Device Type	Light Source	Detection	Channels, nm	Outputs
RunMan (NIR)	7,500	CW	Broadband	GaAs photocells	760 850	Deoxy _(Hb+Mb) Blood volume
NIRO 500 (Hamamatsu)	50,000	CW	Laser diodes	PMT	775 825 850 905	Oxy _(Hb+Mb) Deoxy _(Hb+Mb) Cyt aa ₃ redox
Oximeter (ISS)	40,000	Phase-modulated	Laser diodes	PMT	750 830	[HbO ₂] [Hb] scattering
Niroxan (Wariar et al.)	10,000	CW	Broadband	PMT	770 820 870	Δ Oxy _(Hb+Mb) Δ Deoxy _(Hb+Mb) Δ Cyt aa ₃ redox(?)

Cost estimate includes optoelectronic device and computer used to display outputs of device. NIRS, near-infrared spectrometry; Mb, myoglobin; Cyt, cytochrome; [HbO₂], oxyhemoglobin concentration; [Hb], Hb concentration; CW, continuous wave; GaAs, gallium arsenide; PMT, photomultiplier tube.

biological absorbances in vitro that are accurate, 3) it can be used on the skeletal muscle of healthy human subjects to produce data that are consistent with NIRS measurements produced by other NIRS devices and with parallel measurements that use other methodologies, 4) it can detect the expected evidences of abnormal patterns of tissue oxygenation and deoxygenation in a human patient with an inborn error of skeletal muscle metabolism that should preclude normal skeletal muscle O₂

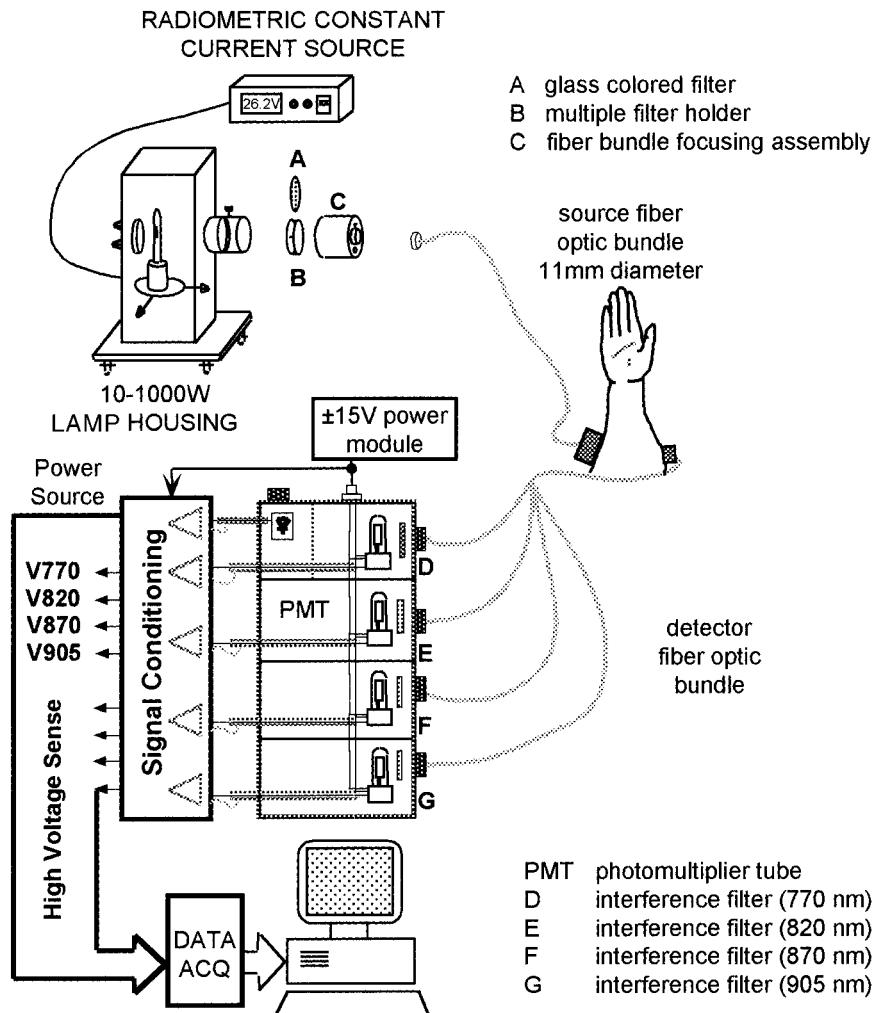
extraction, and 5) the data collected from this patient are of sufficient quality that they may be used as a component of sophisticated clinical neuromuscular diagnosis.

METHODS

System Design

A modular design paradigm was used for construction of the NIRS system (Fig. 1), thereby allowing the flexibility to

Fig. 1. Schematic diagram of overall instrument design. V₇₇₀, V₈₂₀, V₈₇₀, and V₉₀₅, voltages at wavelengths of 770, 820, 870, and 905 nm, respectively.



change the light source intensity, the light source spectral characteristics, the number of wavelengths to be sampled, and the detector wavelengths or sensitivity. A 100-W, quartz tungsten halogen lamp (model 6333, Oriel, Stratford, CT) driven by a constant-current power supply (model 68830, Oriel) was used as the light source. The output of the lamp was filtered using a colored glass filter (model 59545, Oriel) to remove ultraviolet and visible light and then coupled to a fiber-optic bundle (model 77533, Oriel), hereafter called the source fiber bundle, by a fiber bundle-focusing assembly (model 77799, Oriel). Light emerging from tissue was collected using a fiber-optic bundle (detector fiber bundle; Fiber-guide Industries, Stirling, NJ) placed directly over the muscle of interest (flexor digitorum profundus) (3), ~5 cm lateral from the source fiber-optic bundle. The detector fibers were divided into four legs, and light output from each individual leg was band-pass filtered using readily commercially available narrow-band interference filters at wavelengths of 770, 820, 870, and 905 nm (models S10-770-A, S10-820-A, S10-870-A, and S10-905-A, respectively, Corion, Holliston, MA). The 905-nm channel was not used in the present validation. The wavelengths were chosen to cover the near-infrared range of interest over an even spacing (7) and to maximize the sensitivity of absorption changes in response to tissue oxygenation (7, 29). Light outputs of the interference filters were measured in parallel by use of separate gallium-arsenide photocathode photomultiplier tubes (PMTs; model R928, Hamamatsu). PMTs were chosen as optical detectors because of their intrinsically high optical sensitivity. Each PMT was enclosed in light-tight aluminum housing with the inner surfaces coated in black paint, and fiber-to-PMT adapters were constructed as stepped cylinders and fitted onto the enclosures. High-voltage socket power supplies (HC123-01, Hamamatsu) were incorporated inside PMT housings and driven from a ± 15 V regulated power supply. The output currents of each of the PMTs were signal conditioned in parallel; briefly, a current-to-voltage converter converted the PMT output current to a voltage that was amplified and low-pass filtered.

The output voltage of each channel was sampled using a data acquisition system (NI-DAQ-16L, LabView version 3.1, National Instruments, Austin, TX) interfaced to a computer (Macintosh Quadra 700, Apple Computer, Cupertino, CA). All voltage signals were sampled at 10 Hz and filtered using a five-point decimation-smoothing filter. Changes in optical absorption (ΔA) of tissue were calculated at each wavelength from the logarithmic ratio of measured output voltage (V_o) as follows

$$-\Delta \log[V_o - V_{\text{dark}}] \equiv -\log \left[\frac{V_o(t) - V_{\text{dark}}}{V_b - V_{\text{dark}}} \right] = \Delta A(t) \quad (1)$$

The dark voltage (V_{dark}) was the output voltage with no source illumination, and the baseline voltage (V_b) was the output voltage measured from the forearm at rest, before circulatory occlusion or exercise. V_{dark} and V_b were calculated from 30-s averages of the voltage at each wavelength. Therefore, absorption changes were calculated as a function of time, $\Delta A(t)$, with reference to the baseline absorption of tissue (i.e., at rest). As in other optical systems, the accuracy of ΔA is a function of the linearity of the optical detector subsystem and the implicit assumption that lumped system losses remain constant through the duration of the measurement. This is validated in *Optical and Electrical Performance Validation*.

The measured changes in optical absorption were converted to changes (Δ) in concentrations of oxygenated (Hb + Mb) and deoxygenated (Hb + Mb) [$\Delta \text{oxy}_{(\text{Hb} + \text{Mb})}$] and

oxidized cytochrome aa_3 ($\Delta \text{ox-cyt}$) on the basis of the method of Wray et al. (29). Briefly, by making the assumption that the change in absorption at each wavelength is the linear combination of the three changing concentrations (i), Eq. 2 results, where $\epsilon_{\lambda,i}$ is the molar extinction coefficient of *chromophore i* at wavelength λ , ΔC_i is the change in concentration of *chromophore i*, and d is the optical pathlength. Thus the measured absorptions were multiplied by a matrix of NIRS coefficients obtained by substituting the intrinsic molar extinction coefficients of $\Delta \text{oxy}_{(\text{Hb} + \text{Mb})}$ and $\Delta \text{deoxy}_{(\text{Hb} + \text{Mb})}$ (29) and oxidized minus reduced absorption coefficients of cytochrome aa_3 (7) into Eq. 2 and inverting the matrix (Eq. 3). This provides three equations for the three unknowns

$$\Delta A_\lambda = \sum_i \epsilon_{\lambda,i} \cdot \Delta C_i \cdot d \quad (2)$$

Because d requires more sophisticated measuring techniques and was not measured in vivo, $\Delta \text{oxy}_{(\text{Hb} + \text{Mb})}$ and $\Delta \text{deoxy}_{(\text{Hb} + \text{Mb})}$ were expressed in units of millimolar times centimeters. Although the ox-cyt signal could be calculated from Eq. 3, these calculations are not presented, because we do not have a satisfactory combination of in vitro and in vivo validations for these signals. Additionally, the changes in total Hb (ΔtHb) were calculated by summing the $\Delta \text{oxy}_{(\text{Hb} + \text{Mb})}$ and $\Delta \text{deoxy}_{(\text{Hb} + \text{Mb})}$ signals.

Thus Eq. 2 states that the change in absorption at a given λ is equal to the sum of the molar extinction coefficients at that given wavelength times the change in concentration of the chromophore exhibiting the absorption times the mean pathlength traveled by the photons absorbed by that chromophore

$$\begin{bmatrix} \Delta \text{oxy}_{(\text{Hb} + \text{Mb})} \\ \Delta \text{deoxy}_{(\text{Hb} + \text{Mb})} \\ \Delta \text{ox-cyt} \end{bmatrix} \cdot d = \begin{bmatrix} -0.459 & -2.260 & 2.979 \\ 1.211 & -1.140 & 0.210 \\ -0.208 & 1.660 & -1.240 \end{bmatrix} \begin{bmatrix} \Delta A_{770} \\ \Delta A_{820} \\ \Delta A_{870} \end{bmatrix} \quad (3)$$

Thus, on the basis of the intrinsic optical-physical characteristics described in Eq. 2, Eq. 3 displays the matrix operators (including inversion of the extinction coefficients used) to make the calculations we present. Although we chose previously published extinction coefficients, the validity of our choices of extinction coefficients (in the context of our instrument design and application to the collection of optical signals from the human forearm) required in vitro as well as in vivo validation.

Optical and Electrical Performance Validation

The absorption linearity measurement was determined by cascading two filter wheels containing neutral density filters of known absorption and placing them between the source and detector fiber bundles. Percent linearity over the range of 3–5 optical density units (OD; this absorption range was chosen by comparing the voltage outputs from the human forearm with neutral density filters) was 3% and was within manufacturer specification of accuracy for the filters. Because such an in vitro method is not sensitive to small deviations from linearity, two additional approaches were used: 1) in vitro measurements of Hb solutions of known oxygenation and 2) comparison of the ΔtHb signal with blood volume measured in vivo by strain-gauge plethysmography.

System outputs were also evaluated for drift and random noise. Absorptions at the three wavelengths were measured at 4 OD for 1 h, and a 5-min moving-average filter was imposed to significantly attenuate random noise during the measurement of drift. System drift was defined as the maximum deviation of the absorption from its starting reference value

in 1 h. Random noise was estimated as the standard deviation of absorption over a duration equal to 5 min at 4 OD.

System Validation

In vitro. To validate the $\Delta\text{oxy}_{(\text{Hb} + \text{Mb})}$ and $\Delta\text{deoxy}_{(\text{Hb} + \text{Mb})}$ signal outputs of the NIRS system *in vitro*, an oxygenated Hb solution was prepared (29) from human erythrocytes, and its concentration was measured using the CO-oximeter add-on unit (model IL482, Instrumentation Laboratories, Norwood, MA) of a standard laboratory blood gas analyzer. The Hb solution was diluted to the physiological concentration range of 30–420 mM and placed in a custom 1-in. vial between the source and detector fibers of the NIRS system, and sodium dithionite was added to completely reduce HbO_2 (30). NIRS measurements were then compared with tHb measured using the CO-oximeter.

In vivo: measurement of skeletal muscle O_2 availability. *In vivo* validations of the system were performed in humans on skeletal muscle during rest, ischemia, hyperemia, and exercise. After the subjects gave informed consent to the protocol (approved by the Institutional Review Boards of Presbyterian Hospital and the University of Texas Southwestern Medical Center), we performed a series of *in vivo* validation studies on a total of 12 healthy human subjects. To assess the ability of this device to detect disorders of skeletal muscle oxidative metabolism, we compared these results with those collected from a well-characterized (23) patient with coenzyme Q_{10} deficiency, a deficiency in one of the enzymes of the electron transport chain. In the conduct of these *in vivo* validations, five of the healthy subjects participated during ischemia and exercise and five during venous occlusion; three healthy subjects were controls for the coenzyme Q_{10} -deficient patient.

The coenzyme Q_{10} -deficient patient was chosen for study, because the underlying biochemical defect and the pathophysiology of large muscle exercise have been well characterized (23). Because this enzyme deficiency severely limits muscle oxidative phosphorylation, systemic arteriovenous difference is virtually unchanged from rest during peak exercise, consistent with severely impaired O_2 extraction by working muscle. Thus we would expect that the tissue deoxygenation normally seen in healthy subjects during exercise would not occur in this patient.

Statistics

$\Delta\text{oxy}_{(\text{Hb} + \text{Mb})}$ and $\Delta\text{deoxy}_{(\text{Hb} + \text{Mb})}$ are usually expressed in units of millimolar times centimeters as changes from baseline values (defined as 0) during rest. Differences between calculated means (of the form x_i vs. x_j) were determined by two-tailed group *t*-test (19). Statistical significance was defined for $P < 0.05$. Rates of decline during ischemia were calculated from a linear regression into the 1st min of the $\Delta\text{oxy}_{(\text{Hb} + \text{Mb})}$ decay after circulatory occlusion. The time to ischemic steady state for $\Delta\text{oxy}_{(\text{Hb} + \text{Mb})}$ was defined as the time elapsed from circulatory occlusion to time beyond which continuing circulatory occlusion produced no change in the magnitude of the signal.

RESULTS

Optical Performance

Signal stability and random noise. The measured output drift was 0.004, 0.001, and 0.004 OD/h at wavelengths of 770, 820, and 870 nm, respectively. Random noise standard deviations were measured as 0.005, 0.005, and 0.008 OD at wavelengths of 770, 820, and 870 nm, respectively.

Absorbance linearity. The absorption measured across neutral density filters (ΔA_{meas}) with the custom-designed NIRS device was compared with the manufacturer-specified absorption (ΔA_f) for each filter at the wavelengths of 770, 820, and 870 nm. The least-squares estimates of the slope and intercept of the linear fit at 770 nm [0.97 ± 0.02 and 0.01 ± 0.02 (SE), respectively] were not different ($P > 0.05$) from unity or zero, respectively. Similar results were obtained from the least-squares linear fits to absorptions measured at the other discrete wavelengths. Linearity was 97% when calculated by dividing the maximum difference between the absorption and the least-squares fit by the absorption range of 1.8 OD (20).

In Vitro Validations

Accuracy of Hb oxygenation measurements. The reduction of Hb by use of sodium dithionite produced a decrease in the $\Delta\text{oxy}_{(\text{Hb})}$ signal and an increase in the $\Delta\text{deoxy}_{(\text{Hb})}$ signal. Because of equal and opposite changes in the $\Delta\text{oxy}_{(\text{Hb})}$ and $\Delta\text{deoxy}_{(\text{Hb})}$ signals, variations in ΔtHb were limited to signal fluctuations observed as a result of initial sample stirring. To quantitatively validate the linearity (and accuracy) of the measurement *in vitro*, $\Delta\text{oxy}_{(\text{Hb})}$ and $\Delta\text{deoxy}_{(\text{Hb})}$ were compared with the concentration of ($\text{HbO}_2 + \text{Hb}$) measured using a standard clinical blood laboratory CO-oximeter. A linear response was observed (Fig. 2) between the NIRS and CO-oximeter measurements, with maximum deviation of the $\Delta\text{oxy}_{(\text{Hb})}$ and $\Delta\text{deoxy}_{(\text{Hb})}$ signals from the line of identity being 5 and 2% (of the range), respectively.

In Vivo Validations in Normal Healthy Human Skeletal Muscle

Muscle ischemia. Data were collected during 5 min of rest. Circulatory occlusion was then imposed, and the outputs of the NIRS algorithm indicated that, immedi-

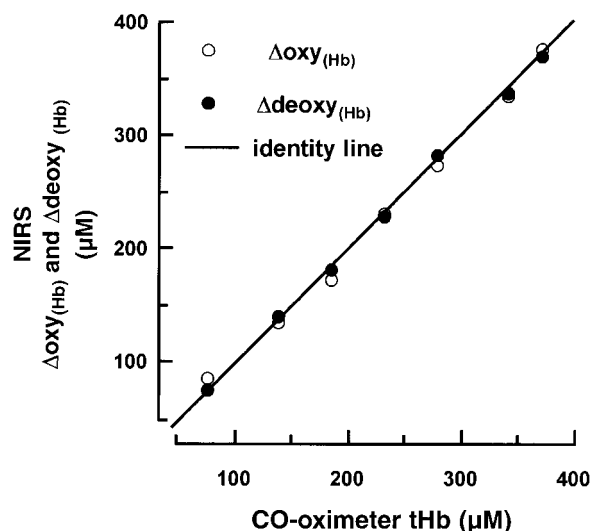


Fig. 2. Validation of measurements of changes in oxy- and deoxyhemoglobin [$\Delta\text{oxy}_{(\text{Hb})}$ and $\Delta\text{deoxy}_{(\text{Hb})}$] in Hb isolated from human blood by near-infrared spectrometry (NIRS) with measurements made on same Hb by a CO-oximeter. Maximum deviation from line of identity was 5 and 2% for $\Delta\text{oxy}_{(\text{Hb})}$ and $\Delta\text{deoxy}_{(\text{Hb})}$, respectively. tHb, total Hb.

ately after arterial occlusion, the $\Delta\text{oxy}_{(\text{Hb}+\text{Mb})}$ signal decreased below its rest control value (Fig. 3), concurrent with a proportional increase in the $\Delta\text{deoxy}_{(\text{Hb}+\text{Mb})}$ signal, and therefore produced no net change ($P > 0.05$) in the $\Delta\text{tHb}_{\text{volume}}$ signal.

Muscle hyperemia. After the muscle oxygenation reached a stable nadir, the occluding cuff was deflated. At this point (Fig. 3), the $\Delta\text{oxy}_{(\text{Hb}+\text{Mb})}$ signal increased and the $\Delta\text{deoxy}_{(\text{Hb}+\text{Mb})}$ signal decreased rapidly. This led to an increase of $\Delta\text{tHb}_{\text{volume}}$ because of a greater increase in the $\Delta\text{oxy}_{(\text{Hb}+\text{Mb})}$ vs. the $\Delta\text{deoxy}_{(\text{Hb}+\text{Mb})}$ signal, which reached its maximum value within 1 min after cuff release, and then a return to control level within 7 min.

Muscle rhythmic exercise. Immediately at the onset of rhythmic handgrip (RHG) exercise (5 s of static finger flexion at 33% of the maximal voluntary contractile force alternated with 5 s of rest), there was an immediate decrease in the average $\Delta\text{oxy}_{(\text{Hb}+\text{Mb})}$ signal by ~ 0.3 mM·cm within the first 30 s (over the first 3 exercise-rest cycles) after the onset of exercise (Fig. 4) and then a stable and repeatable cycling of the signal (at a frequency of ~ 0.1 Hz), which was the same period as that of the RHG. The 0.1-Hz transient decreases of the $\Delta\text{oxy}_{(\text{Hb}+\text{Mb})}$ signal were coincident with the correspond-

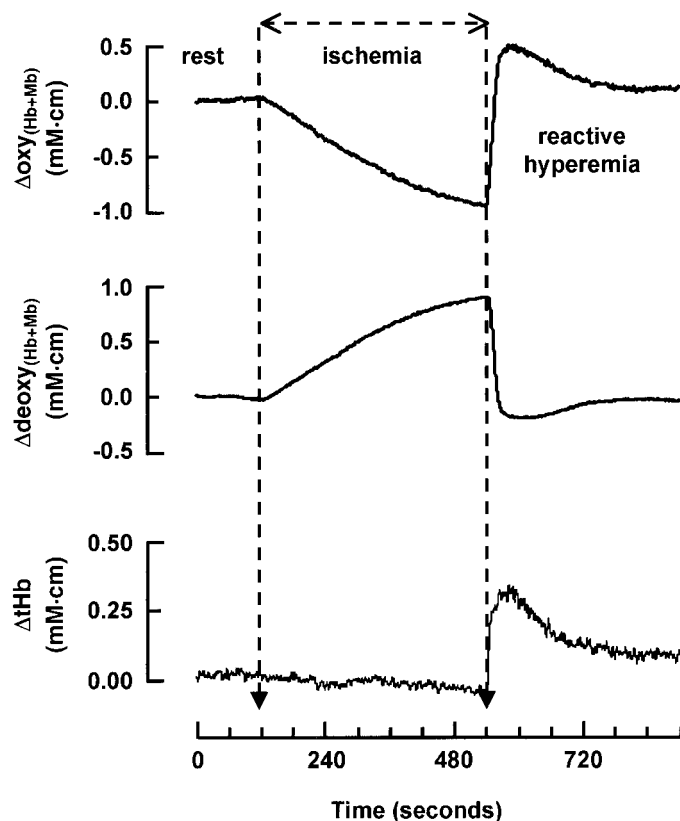


Fig. 3. NIRS measurement (mean of 5 normal, healthy subjects) from human forearm during circulatory occlusion. Data were collected during periods of control (rest), ischemia, reactive hyperemia, and return to control. Changes in sums of oxyhemoglobin and oxymyoglobin [$\Delta\text{oxy}_{(\text{Hb}+\text{Mb})}$] and deoxyhemoglobin and deoxymyoglobin [$\Delta\text{deoxy}_{(\text{Hb}+\text{Mb})}$] were stoichiometric and opposite. No change in summed signal (ΔtHb) could be detected until hyperemia.

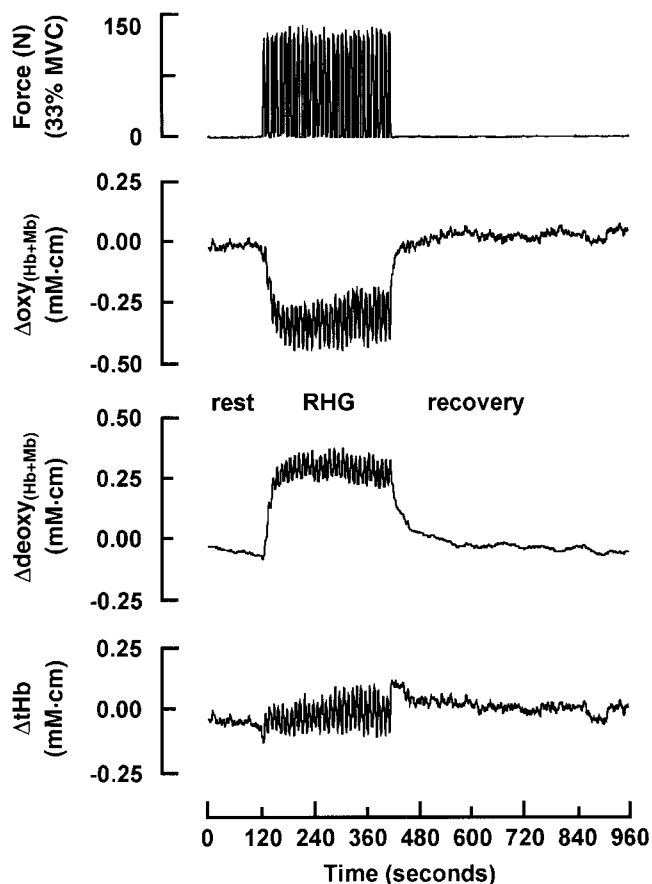


Fig. 4. NIRS measurement (mean of 5 healthy subjects) from human forearm during rhythmic handgrip (RHG) exercise. Data were collected during periods of control, RHG [5 s of contraction at 33% of maximal voluntary contractile force (MVC) alternated with 5 s of rest], and recovery from exercise. Changes in $\Delta\text{oxy}_{(\text{Hb}+\text{Mb})}$ and $\Delta\text{deoxy}_{(\text{Hb}+\text{Mb})}$ were stoichiometric and opposite. No net change in ΔtHb signal could be detected until hyperemia.

ing transient increases in the $\Delta\text{deoxy}_{(\text{Hb}+\text{Mb})}$ signal and the transient increase in force during each contraction.

Movement artifacts. Optical measurements can be very sensitive to movement artifacts. During RHG exercise in normal nonischemic muscle (Fig. 5), the $\Delta\text{oxy}_{(\text{Hb}+\text{Mb})}$ signal contained two components: 1) a decrease in the average or filtered $\Delta\text{oxy}_{(\text{Hb}+\text{Mb})}$ signal over the entire exercise period (Fig. 5C) and 2) cyclical changes during each contraction-relaxation cycle (Fig. 5B). To estimate the contribution of movement artifacts to the above signal, RHG was repeated under two different conditions where tissue oxygenation could be expected to remain constant: 1) normal “loaded” exercise performed after 10 min of ischemia (Fig. 5, D and E) and 2) “no-load” exercise, i.e., exercise (with normal finger flexion activity) performed without resistance to movement (Fig. 6).

With 10 min of ischemia before RHG exercise, the average $\Delta\text{oxy}_{(\text{Hb}+\text{Mb})}$ signal reached a steady-state nadir (normalized to -1.0 in Fig. 5, D and E). Therefore, because exercise in such a condition of an ischemic nadir could not cause a further reduction in the tissue oxygenation, any cyclical signal changes detected during RHG exercise in this condition could only arise from

movement artifacts. This amplitude of cyclical $\Delta\text{oxy}_{(\text{Hb}+\text{Mb})}$ signal changes during ischemic exercise (Fig. 5), expressed as a percentage of the filtered $\Delta\text{oxy}_{(\text{Hb}+\text{Mb})}$ change during RHG exercise, performed at the same intensity but without circulatory occlusion, was 16%. Similarly, the amplitude of cyclical $\Delta\text{oxy}_{(\text{Hb}+\text{Mb})}$ signal changes during ischemic exercise, as a percentage of the cyclical $\Delta\text{oxy}_{(\text{Hb}+\text{Mb})}$ changes during RHG exercise, was 34%.

Similarly, during unloaded finger flexion exercise (Fig. 6), there was no distinct change in the average $\Delta\text{oxy}_{(\text{Hb}+\text{Mb})}$ signal. Thus this procedure could be used to estimate the contribution to the overall signal from movement with tissue “normally” oxygenated. Additionally, there was no distinctly different cyclical $\Delta\text{oxy}_{(\text{Hb}+\text{Mb})}$ signal during no-load exercise.

Validation of tHb with venous occlusion plethysmography. During venous occlusion, the initial rate of increase of total limb cross-sectional volume (ΔtV_l) during the first 20 s, measured using strain-gauge plethysmography, was $4.3 \pm 0.7 \text{ ml} \cdot 100 \text{ ml tissue}^{-1} \cdot \text{min}^{-1}$. The ΔtV_l was the same for all venous occlusion pressures (20–70 mmHg; Fig. 7). Each of the signals was normalized, at their respective occlusion pres-

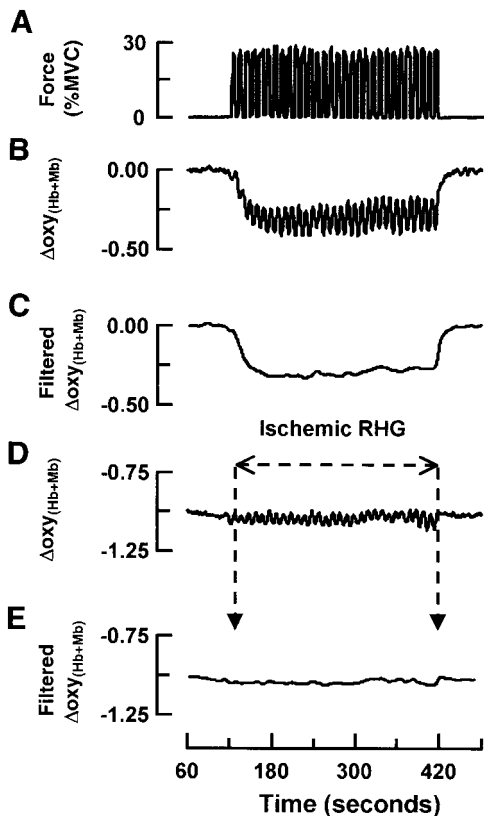


Fig. 5. NIRS measurement (mean of 5 healthy subjects) from human forearm during RHG exercise (5 s of contraction at 33% MVC alternated with 5 s of rest). A: force; B: $\Delta\text{oxy}_{(\text{Hb}+\text{Mb})}$; C: $\Delta\text{oxy}_{(\text{Hb}+\text{Mb})}$ data from B filtered using a digital 10-s moving-average filter to remove cyclical changes of $\text{oxy}_{(\text{Hb}+\text{Mb})}$ during exercise; D: $\Delta\text{oxy}_{(\text{Hb}+\text{Mb})}$ during same type of exercise protocol but performed after 10 min of vascular occlusion so that there would be no further decline in $\Delta\text{oxy}_{(\text{Hb}+\text{Mb})}$; E: $\Delta\text{oxy}_{(\text{Hb}+\text{Mb})}$ data from D filtered using a digital 10-s moving-average filter.

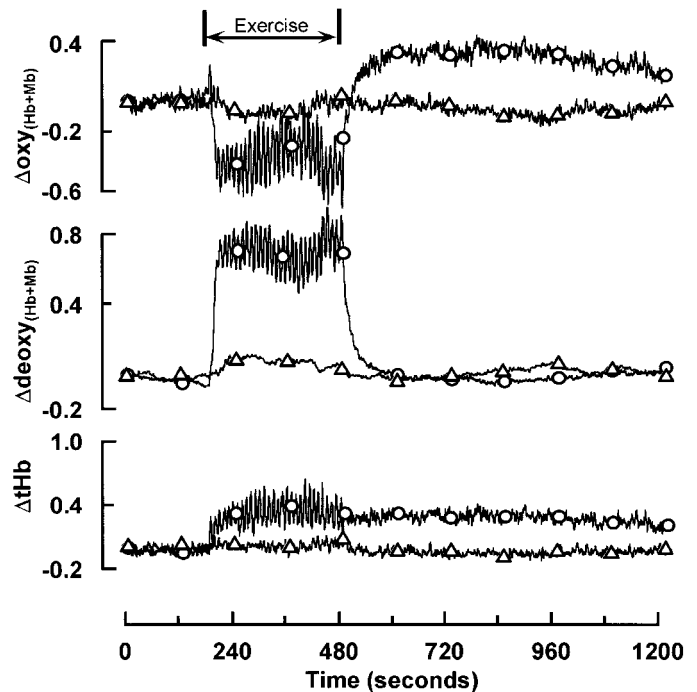


Fig. 6. A comparison of $\Delta\text{oxy}_{(\text{Hb}+\text{Mb})}$ and $\Delta\text{deoxy}_{(\text{Hb}+\text{Mb})}$ measured during RHG exercise performed with (○) and without (△) force generation. In exercise performed without a load, there would be normal motional component of finger flexion activity but no exercise-mediated decline in $\Delta\text{oxy}_{(\text{Hb}+\text{Mb})}$. These data were used to estimate magnitude of metabolic vs. nonmetabolic (motional) components of observed NIRS signals during RHG exercise.

sures, to the total signal change. Expressed in this manner, the ΔtV_l was $2.3 \pm 0.3\%/s$. The changes in total Hb volume ($\Delta\text{tHb}_{\text{volume}}$) were linearly correlated with the change in total volume (ΔtV ; $r^2 = 0.99$; Fig. 8). Likewise, the initial rate of increase of tHb_{volume} (ΔtHb_l), normalized to the maximum signal change at each occlusion pressure, was $2.3 \pm 0.5\%/s$ and was not different from ΔtV_l . With cuff deflation after venous occlusion, ΔtV and $\Delta\text{tHb}_{\text{volume}}$ decreased in a characteristic biphasic manner, with a rapid decline lasting ~ 5 s followed by a slower decline to rest values over ~ 1 min (Fig. 7).

In Vivo Validations in Skeletal Muscle of the Coenzyme Q₁₀-Deficient Patient

Muscle ischemia. Circulatory arrest produced an immediate decline in the $\Delta\text{oxy}_{(\text{Hb}+\text{Mb})}$ signal. The initial rate of decline of $\Delta\text{oxy}_{(\text{Hb}+\text{Mb})}$ in the patient ($-0.0076 \text{ mM} \cdot \text{cm} \cdot \text{s}^{-1}$ or 56%/min) was not different from that in healthy subjects. It took about the same time (218 s) to reach an ischemic nadir, and the level of the ischemic steady-state nadir was about the same as in healthy subjects. Again, as in healthy subjects, circulatory occlusion resulted in an increase in the $\Delta\text{deoxy}_{(\text{Hb}+\text{Mb})}$ signal that was approximately stoichiometric, so that there was no net change in ΔtHb .

Muscle exercise. In contrast to healthy subjects, RHG exercise caused an increase in $\Delta\text{oxy}_{(\text{Hb}+\text{Mb})}$ above rest level (Fig. 9). During the first 110 s after the onset of RHG exercise, the average $\Delta\text{oxy}_{(\text{Hb}+\text{Mb})}$ signal reached a

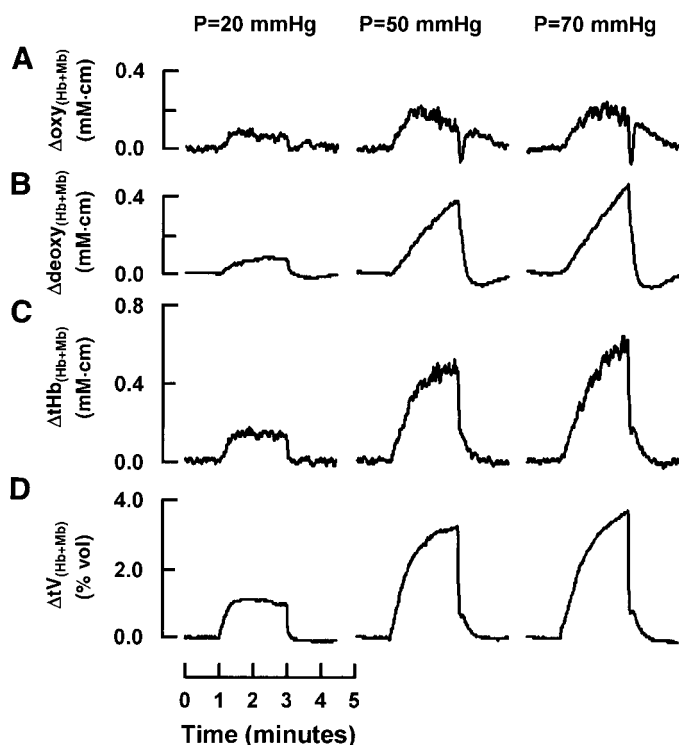


Fig. 7. Validation of changes (mean of 5 healthy subjects) in $\Delta oxy_{(Hb+Mb)}$ and $\Delta deoxy_{(Hb+Mb)}$ measured in human forearm by NIRS by comparing their summed signal (ΔtHb_{volume}) with changes in total limb volume (ΔtV) measured simultaneously using venous occlusion plethysmography. Limb volume changes were induced by subdiastolic congestion with an occlusion cuff inflated to pressures (P) of 20, 50, and 70 mmHg. In each case, initial rate of increase of total limb cross-sectional volume (ΔtV_i) during first 20 s was not different from initial rate of increase of ΔtHb_i normalized to maximum signal change. With cuff deflation after venous occlusion, ΔtV and ΔtHb decreased in a characteristic biphasic manner, with a rapid decline lasting ~5 s, then a slower decline to rest values over ~1 min.

peak value of 24.5% above rest level [with use of the arbitrary range where $0 \equiv \Delta oxy_{(Hb+Mb)}$ at rest and $100 \equiv \Delta oxy_{(Hb+Mb)}$ at the ischemic nadir]. This increase in the average $\Delta oxy_{(Hb+Mb)}$ signal was accompanied by a

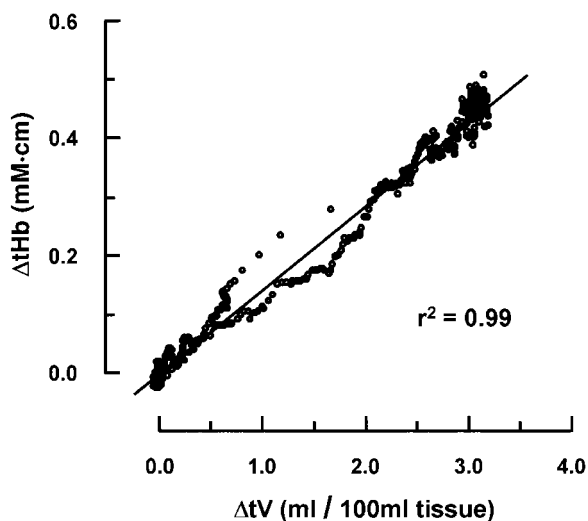


Fig. 8. Correlation coefficient between NIRS ΔtHb_{volume} and ΔtV from data in Fig. 6.

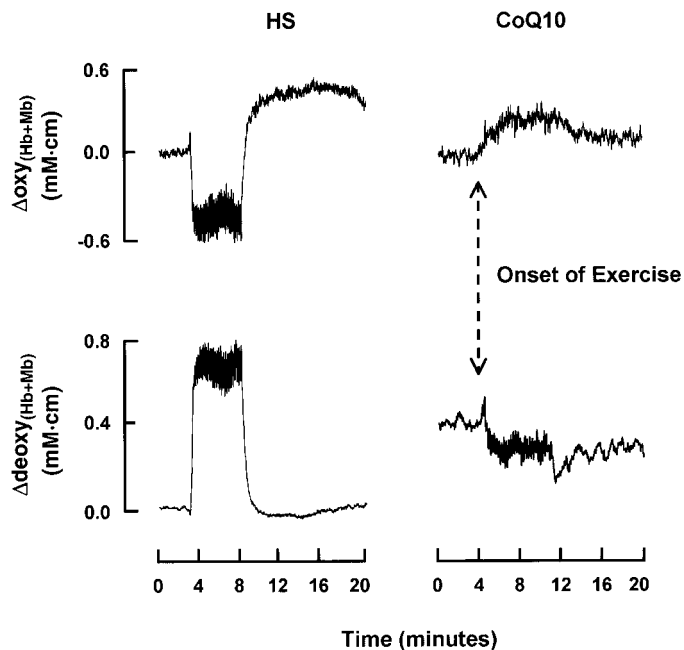


Fig. 9. Comparison of NIRS data collected during 5 min of maximal RHG exercise from a healthy subject (HS) with data collected from a patient deficient in skeletal muscle coenzyme Q_{10} (CoQ10). In healthy subject, decline in $\Delta oxy_{(Hb+Mb)}$ and increase in $\Delta deoxy_{(Hb+Mb)}$ reached a steady state within first 3 contraction-relaxation cycles. In contrast, in coenzyme Q_{10} -deficient patient, there was a net increase in $\Delta oxy_{(Hb+Mb)}$ and decrease in $\Delta deoxy_{(Hb+Mb)}$. This increase in mean average $\Delta oxy_{(Hb+Mb)}$ signal indicates a net increase in perfusion over extraction, consistent with previously documented absence of increase in systemic arteriovenous O_2 difference and exaggerated systemic O_2 transport relative to O_2 utilization during cycle exercise.

decrease in the $\Delta deoxy_{(Hb+Mb)}$ signal and was very different from that in healthy subjects. Because the increase in the $\Delta oxy_{(Hb+Mb)}$ signal was greater than in the $\Delta deoxy_{(Hb+Mb)}$ signal, a small net increase in ΔtHb_{volume} was detected in the coenzyme Q_{10} -deficient patient during RHG exercise.

DISCUSSION

The inherent difficulties in making NIRS measurements of internal physiological systems often have caused the focus of much of this work to be technological. Most of the engineering approaches to making these measurements are focused on designing as thorough a measurement system as possible (5, 9, 13), at the cost of instrument expense and inflexibility, or on designing a simple and inexpensive system that can be used to examine exercising skeletal muscle, possibly at the additional cost of sensitivity (15, 16, 18). We describe an intermediate approach that is relatively inexpensive to construct and relatively simple to implement and produces adequate and stable signal-to-noise ratio. It is clear that our implementation of NIRS methodology can successfully monitor skeletal muscle metabolism in exercising human skeletal muscle, that the results can be validated in vitro and in vivo, and that the results can be extended to diagnose clinical conditions. Thus we believe that our implementation of NIRS technology will provide a much more widespread

availability to study skeletal muscle oxidative metabolism.

Optical and Electrical Performance Validation

Signal stability. Our estimate of signal stability is a combination of the effect of random noise (electrical and optical) and the overall stability of the system. Over a 60-min period, the sum total of the absolute value of the system drift in the three channels combined was $\sim 1\%$ of the absolute value of the sum of the absorbances in all channels during ischemia. Thus it is unlikely that signal instability contributes measurable error to our calculations of tissue oxygenation.

Error propagation analysis of the NIRS system. Beyond stability and the random noise of the absorption, a more rigorous approach to evaluating system noise is to calculate the magnitude of the error of the measurement itself. Because absorption is not the final measurement, it is more valuable to calculate the errors propagated in the process of actually calculating $\Delta\text{oxy}_{(\text{Hb}+\text{Mb})}$ and $\Delta\text{deoxy}_{(\text{Hb}+\text{Mb})}$. On the basis of our algorithm (Eq. 3), the worst-case propagated errors were calculated from the root-square sum of the random noise at each wavelength. Therefore, the net worst-case drift (D) for $\Delta\text{oxy}_{(\text{Hb}+\text{Mb})}$ and $\Delta\text{deoxy}_{(\text{Hb}+\text{Mb})}$ is

$$\begin{aligned} D_{\text{oxy}(\text{Hb})} &= \sqrt{(-0.459 \times 0.004)^2 + (-2.260 \times 0.001)^2} \\ &\quad + (2.979 \times 0.004)^2} \\ &= 0.012 \text{ mM} \cdot \text{cm} \end{aligned}$$

$$\begin{aligned} D_{\text{deoxy}(\text{Hb})} &= \sqrt{(1.1211 \times 0.004)^2 + (-1.140 \times 0.001)^2} \\ &\quad + (0.210 \times 0.004)^2} \\ &= 0.005 \text{ mM} \cdot \text{cm} \end{aligned}$$

Similarly, the net worst-case random noise for $\Delta\text{oxy}_{(\text{Hb}+\text{Mb})}$ and $\Delta\text{deoxy}_{(\text{Hb}+\text{Mb})}$ is

$$\begin{aligned} \sigma_{\text{oxy}(\text{Hb})} &= \sqrt{(-0.459 \times 0.005)^2 + (-2.260 \times 0.005)^2} \\ &\quad + (2.979 \times 0.008)^2} \\ &= 0.026 \text{ mM} \cdot \text{cm} \end{aligned}$$

$$\begin{aligned} \sigma_{\text{deoxy}(\text{Hb})} &= \sqrt{(1.1211 \times 0.004)^2 + (-1.140 \times 0.001)^2} \\ &\quad + (0.210 \times 0.004)^2} \\ &= 0.008 \text{ mM} \cdot \text{cm} \end{aligned}$$

Together, the drift (D) noise is only about one-half the random noise standard deviation (σ): for $\Delta\text{oxy}_{(\text{Hb}+\text{Mb})}$ $\sim 3\%$ (0.026 mM·cm per mM·cm) of the total signal change during ischemia and $\sim 9\%$ (0.026 mM·cm per 0.3 mM·cm) of the signal change during maximal RHG exercise.

Absorbance linearity. The linearity of the absorption measurement was defined as the maximum ΔA_{meas} from a least-squares line fit with neutral density filters (ΔA_f). On the basis of the slope and intercept of the straight line relating ΔA_{meas} with ΔA_f , the 97% linearity

(over 1.8 OD) and zero intercept indicated near-perfect linearity.

In Vitro Validations

Hb cuvette and accuracy data. Because the NIRS outputs were so consistent with CO-oximeter outputs, with negligible cross talk between $\Delta\text{oxy}_{(\text{Hb})}$ and $\Delta\text{deoxy}_{(\text{Hb})}$, the NIRS algorithm (Eq. 3) was considered valid in converting net O_2 -dependent absorption change to the individual absorptions of $\Delta\text{oxy}_{(\text{Hb})}$ and $\Delta\text{deoxy}_{(\text{Hb})}$ in vitro. The only corrections remaining would be those for the actual pathlength in vivo (structural impediments to photon migration plus changes in source-detector orientation during exercise) and differential changes in the concentrations of individual chromophores not part of the derivation of the algorithm coefficients. We believe that most of these are accounted for in our in vivo validations.

In Vivo Validations

Measurement of tissue oxygenation by NIRS is simple but complex. It is simple, because the biophysics of optical absorption of photons by chromophores is well understood. It is complex, because 1) the absorbances of Hb and Mb are indistinguishable (7, 22), 2) the absorbances of Hb in separate anatomic compartments (relative sizes of “arterial,” “capillary,” or “venous” spaces) are detected and displayed as a summed signal, 3) there is interaction between blood flow and perfusion, 4) Hb oxygenation changes monotonically from the arterial to the capillary to the venous circulation in a complex fashion (21), 5) the saturations of Hb and Mb are different and dynamically changing as a function of the rate of O_2 utilization and delivery, and 6) the effect of exercise on the pattern of photon migration is unknown. Taken together, these complications require rigorous biological validations. All our biological validations are based on the use of well-known and inherently simple physiological phenomena and comparisons by independent measures.

Muscle ischemia. During arterial occlusion, the changes in absorption at all the monitored wavelengths were qualitatively consistent with the known absorptions of Hb in vitro (29) and data from other NIRS devices (7). Immediately after arterial occlusion, $\Delta\text{oxy}_{(\text{Hb}+\text{Mb})}$ decreased with an increase in $\Delta\text{deoxy}_{(\text{Hb}+\text{Mb})}$ (Fig. 3). This was reasonable, because ongoing mitochondrial respiration would be expected to gradually deplete the O_2 stores present in Hb and Mb, but the arterial occlusion would fix the amount of tHb. As expected, the sum of $\Delta\text{oxy}_{(\text{Hb}+\text{Mb})}$ and $\Delta\text{deoxy}_{(\text{Hb}+\text{Mb})}$ ($\Delta\text{tHb}_{\text{volume}}$) did not change during arterial occlusion.

The $\Delta\text{oxy}_{(\text{Hb}+\text{Mb})}$ and $\Delta\text{deoxy}_{(\text{Hb}+\text{Mb})}$ signals reached a steady-state nadir after 6–7 min of ischemia, an additional 5 min (ischemic) of RHG exercise (at 33% of maximal voluntary contractile force), and then another 60 s of rest. We found that the $\Delta\text{oxy}_{(\text{Hb}+\text{Mb})}$ and $\Delta\text{deoxy}_{(\text{Hb}+\text{Mb})}$ signals were not different from those after the initial ischemia. So, although this methodology cannot determine absolute concentration of O_2 , we

do know that this was more than twice the time previously calculated to completely deplete the tissue of O_2 (4) and that exercise did not result in any further deoxygenation. Although this may be a condition where the PO_2 in most compartments is nearly equal to zero (4), it is certainly functionally indistinguishable from “zero”; thus we believe it is most justified to call it a “biological zero.”

Meaning of a biological zero. NIRS $\Delta oxy_{(Hb+Mb)}$ and $\Delta deoxy_{(Hb+Mb)}$ signals are composed of some combination of the following chromophore absorbances: Hb in the arterial or prearteriolar space, Hb in the capillary (postarteriole to prevenule) space, Hb in the venous or postvenule space, and Mb in the muscle. Our definition of an ischemic nadir was that the summed oxygenation of these spaces in the field of view was constant at zero or at some nonzero value where the concentration gradient does not exceed the diffusion gradient (6). Our term biological zero cannot be an absolute measure of the real PO_2 in any subcellular space; rather, it means that no combination of blocking supply (ischemia) and increasing demand (muscle contractile activity) causes any further loss of oxygenation from the sum of detected chromophores. We believe this is the functional equivalent to a mean tissue PO_2 lower than the effective Michaelis-Menten constant in vivo of Mb for O_2 (14, 27, 28) and no higher than the functional Michaelis-Menten constant of mitochondria for O_2 , which in vitro has been reported to be <1.0 Torr (25).

Muscle hyperemia. After the muscle oxygenation reached a stable nadir, the occluding cuff was deflated. At this point, the $\Delta oxy_{(Hb+Mb)}$ signal increased and the $\Delta deoxy_{(Hb+Mb)}$ signal decreased rapidly. This led to an increase of ΔtHb because of a greater increase in the $\Delta oxy_{(Hb+Mb)}$ than in the $\Delta deoxy_{(Hb+Mb)}$ signal, which reached its maximum value within 1 min after cuff release (Fig. 3) and then returned to control level within 7 min. We consider this reasonable: a transient excess of arterial blood creating a transient increase in total blood volume.

Muscle rhythmic exercise. During maximal RHG exercise, the $\Delta oxy_{(Hb+Mb)}$ signal decreased until a steady state was reached within 30 s (3 contraction-relaxation cycles). Normalized to the signal change from rest to ischemic steady state, this decline was -32% . The steady-state or average value of $\Delta oxy_{(Hb+Mb)}$ (calculated by a 10-s moving-average filter) remained below rest level until the end of exercise (Fig. 5C). In addition to a decrease in the average $\Delta oxy_{(Hb+Mb)}$, cyclical changes were observed during each contraction-relaxation cycle. The sustained decrease of the $\Delta oxy_{(Hb+Mb)}$ signal during RHG exercise indicated that the high O_2 consumption of muscle during exercise was accommodated by a combination of a net increase in O_2 extraction (oxidative phosphorylation) over delivery (blood flow), possibly in combination with a muscle pump-mediated decrease in total venous volume. Increases in $\Delta deoxy_{(Hb+Mb)}$ were equal and opposite to that of the $\Delta oxy_{(Hb+Mb)}$ signal; therefore, the sum ($\Delta tHb_{\text{volume}}$) remained unchanged.

Estimation of movement artifacts. We calculated the magnitude of movement artifacts to overall oxygenation

measurements during exercise in vivo 1) after 10 min of vascular occlusion, where muscle contraction causes no further tissue deoxygenation (4), and 2) during exercise with no load and, thus, little or no increase in muscle oxidative metabolism.

At the ischemic nadir, RHG exercise produced no further deoxygenation (Fig. 5, D and E), so we could superimpose exercise to estimate the magnitude of movement artifact in and of itself. During RHG exercise performed during this ischemia, the small variations detected in $\Delta oxy_{(Hb+Mb)}$ and $\Delta deoxy_{(Hb+Mb)}$ must have arisen from movement artifacts. The amplitude of cyclical variations (movement artifacts; Fig. 5D) was 16% of total average signal change during RHG exercise (Fig. 5C) and 34% of the cyclical $\Delta oxy_{(Hb+Mb)}$ amplitude during RHG exercise (Fig. 5B). Thus the maximal contribution of movement artifacts to the average oxygenation change during RHG exercise could not be more than about one-third of the total cyclical $\Delta oxy_{(Hb+Mb)}$ amplitude. Because the amplitude of movement artifacts was so much smaller than actual oxygenation changes, it is valid to use this NIRS methodology to monitor skeletal muscle deoxygenation patterns during RHG exercise.

Validation of tHb with venous occlusion plethysmography. As one estimate of the accuracy of the NIRS algorithm, we compared its calculation of total blood volume with an independent measure of blood volume: limb volume measurements made using venous occlusion plethysmography. Our assumption was that if two independent measurements agreed, then they were both measuring the same thing equally incorrectly, they were both getting the same outputs and their summed component errors were exactly equal and offsetting, or they were both correct.

The linear proportionality (Figs. 7 and 8) between $\Delta tHb_{\text{volume}}$ (NIRS) and ΔtV (plethysmography) during subdiastolic venous congestion ($r^2 = 0.99$) means that both are correct within the limits of each methodology. Because these two independent measures produced the same outputs at several different subdiastolic limb congestions, during the ascension to, the steady state at, and the recovery from each of three different occluding pressures (Fig. 7), we are confident that the underlying assumptions (principally the inverse matrix solution and the coefficients in the matrix), taken as a unit, are reasonable. Moreover, because our implementation of NIRS in this setting should only detect changes in concentration of Hb, our results suggest that, during acute limb congestions, the changes in limb volume measured by strain-gauge plethysmography are dominated by the change in limb blood volume and that any accompanying changes in limb vs. optode geometry are negligible in the calculation of tHb by NIRS.

Skeletal muscle coenzyme Q_{10} deficiency. We used our NIRS system to monitor muscle oxygenation in a well-characterized patient with a deficiency of skeletal muscle coenzyme Q_{10} (1, 2, 23). This patient had impaired oxidative metabolism in skeletal muscle from a reduction in coenzyme Q_{10} concentration to $<25\%$ of normal, impairing the catalytic activities of complexes

I-II and I-III. During large muscle exercise, patients with such mitochondrial myopathies typically exhibit premature fatigue and exercise intolerance. The impairment in muscle oxidative phosphorylation is so severe that there is no increase in the arteriovenous O_2 difference during exercise.

We found that muscle O_2 extraction during rest was not different from that of healthy subjects, consistent with previous whole body O_2 consumption measurements (23). In contrast, although this patient exhibited a cyclic pattern of tissue oxygenation in synchrony with the pattern of RHG exercise, the $\Delta oxy_{(Hb+Mb)}$ (Fig. 9) increased immediately at the onset of exercise. This increase in the average $\Delta oxy_{(Hb+Mb)}$ signal indicates a net increase in perfusion over extraction, consistent with the previously documented absence of any increase in systemic arteriovenous O_2 difference and exaggerated systemic O_2 transport relative to O_2 utilization during cycle exercise (23).

Summary

These data demonstrate clearly the value of NIRS measurement, in that it provides a completely noninvasive measure of these summed signals with extremely high time resolution. We have presented a system design that provides signal accuracy, stability, and sensitivity in combination with detection flexibility at relatively low cost and simple implementation. We have validated its outputs and demonstrated its utility in vivo in healthy control subjects as well as in a well-characterized human patient with skeletal muscle coenzyme Q_{10} deficiency. We believe that use of such a system can become of widespread utility for routine clinical diagnoses as well as for the study of the interactions between O_2 delivery and utilization in human skeletal muscle.

We acknowledge Dr. Benjamin D. Levine for overall support of this research; the facility support and intellectual contributions of Drs. Chun-Sing Orr, Robert W. Parkey, Craig R. Malloy, Evelyn E. Babcock, Robert C. Eberhart, and Doyle Hawkins; and Karen Aayad, Paul R. Anderson, Karen Chafee, Marguerite Gunder, Iris Lin, and Phil Wyrick for technical assistance.

This research was supported by the Presbyterian Hospital of Dallas, National Institutes of Health Biotechnology Research Facility Grant P41-RR-02584, and National Aeronautics and Space Administration Grant NAGW3582 and by the Department of Veterans Affairs (R. G. Haller). R. Wariar was supported by the Presbyterian Hospital of Dallas.

Address for reprint requests and other correspondence: L. A. Bertocci, Institute for Exercise and Environmental Medicine, Presbyterian Hospital of Dallas, 7232 Greenville Ave., Dallas, TX 75231 (E-mail: bertoccl@phs-care.org).

Received 18 August 1998; accepted in final form 14 September 1999.

REFERENCES

1. **Bank, W., and B. Chance.** Diagnosis of defects in oxidative muscle metabolism by non-invasive tissue oximetry. *Mol. Cell. Biochem.* 174: 7–10, 1997.
2. **Bank, W., and B. Chance.** An oxidative defect in metabolic myopathies: diagnosis by noninvasive tissue oximetry. *Ann. Neurol.* 36: 830–837, 1994.
3. **Bertocci, L. A., R. G. Haller, S. F. Lewis, J. L. Fleckenstein, and R. L. Nunnally.** Abnormal high-energy phosphate metabolism in human muscle phosphofructokinase deficiency. *J. Appl. Physiol.* 70: 1201–1207, 1991.
4. **Blei, M. L., K. E. Conley, and M. J. Kushmerick.** Separate measures of ATP utilization and recovery in human skeletal muscle. *J. Physiol. (Lond.)* 465: 203–222, 1993.
5. **Cheatle, T. R., L. A. Potter, M. Cope, and D. T. Delpy.** Near-infrared spectroscopy in peripheral vascular disease. *Br. J. Surg.* 78: 405–408, 1991.
6. **Clark, A., Jr., P. A. A. Clark, R. J. Connett, T. E. J. Gayeski, and C. R. Honig.** How large is the drop in Po_2 between cytosol and mitochondrion? *Am. J. Physiol. Cell Physiol.* 252: C583–C587, 1987.
7. **Cope, M., and D. T. Delpy.** System for long-term measurement of cerebral blood and tissue oxygenation on newborn infants by near-infrared transillumination. *Med. Biol. Eng. Comput.* 26: 289–294, 1988.
8. **Delpy, D. T., M. Cope, P. van der Zee, S. Arridge, S. Wray, and J. Wyatt.** Estimation of optical pathlength through tissue from direct time of light measurement. *Phys. Med. Biol.* 33: 1433–1442, 1988.
9. **Elwell, C. E.** *A Practical User's Guide to Near-Infrared Spectroscopy.* London: Hamamatsu Photonics, 1995.
10. **Hampson, N. B., and C. A. Piantadosi.** Near-infrared monitoring of human skeletal muscle oxygenation during forearm ischemia. *J. Appl. Physiol.* 64: 2449–2457, 1988.
11. **Hansen, J., G. D. Thomas, S. A. Harris, W. J. Parsons, and R. G. Victor.** Differential sympathetic neural control of oxygenation in resting and exercising human skeletal muscle. *J. Clin. Invest.* 98: 584–596, 1996.
12. **Jöbsis, F. F., J. H. Keizer, J. C. LaManna, and M. Rosenthal.** Reflectance spectrophotometry of cytochrome aa_3 in vivo. *J. Appl. Physiol.* 43: 858–872, 1977.
13. **Jöbsis-VanderVliet, F. F., C. Piantadosi, A. A. Sylvia, L. S. Lucas, and K. H. Keizer.** Near-infrared monitoring of cerebral oxygen sufficiency. I. Spectra of cytochrome c oxidase. *Neurol. Res.* 10: 7–17, 1988.
14. **Kreutzer, U., and T. Jue.** Critical intracellular O_2 in myocardium as determined by 1H nuclear magnetic resonance signal of myoglobin. *Am. J. Physiol. Heart Circ. Physiol.* 268: H1675–H1681, 1995.
15. **Mancini, D. M.** Application of near-infrared spectroscopy to the evaluation of exercise performance and limitations in patients with heart failure. *J. Biomed. Optics* 2: 22–30, 1997.
16. **Mancini, D. M., L. Bolinger, H. Li, K. Kendrick, B. Chance, and J. R. Wilson.** Validation of near-infrared spectroscopy in humans. *J. Appl. Physiol.* 77: 2740–2747, 1994.
17. **Matcher, S. J., C. E. Elwell, C. E. Cooper, M. Cope, and D. T. Delpy.** Performance comparison of several published tissue near-infrared spectroscopy algorithms. *Anal. Biochem.* 227: 54–68, 1995.
18. **McCully, K. K., S. Iotti, K. Kendrick, Z. Wang, J. D. Posner, J. Leigh, Jr., and B. Chance.** Simultaneous in vivo measurements of HbO_2 saturation and PCr kinetics after exercise in normal humans. *J. Appl. Physiol.* 77: 5–10, 1994.
19. **Neter, J., W. Wasserman, and M. H. Kutner.** *Applied Linear Statistical Models.* Boston: Irwin, 1990.
20. **Norton, H. N.** *Handbook of Transducers.* Englewood Cliffs, NJ: Prentice-Hall, 1989.
21. **Segal, S. S.** *Convection, Diffusion and Mitochondrial Utilization of Oxygen During Exercise.* Dubuque, IA: Brown and Benchmark, 1992.
22. **Seiyama, A., O. Hazeki, and M. Tamura.** Noninvasive quantitative analysis of blood oxygenation in rat skeletal muscle. *J. Biochem.* 103: 419–424, 1988.
23. **Sobreira, C., M. Hirano, S. Shanske, R. K. Keller, R. G. Haller, E. Davidson, F. M. Santorelli, A. F. Miranda, D. S. Mojon, A. A. Barriera, M. P. King, and S. DiMauro.** Mitochondrial encephalomyopathy with coenzyme Q_{10} deficiency. *Neurology* 48: 1238–1243, 1997.
24. **Tamura, M., O. Hazeki, S. Nioka, and B. Chance.** In vivo study of tissue oxygen metabolism using optical and nuclear magnetic resonance spectroscopies. *Annu. Rev. Physiol.* 51: 813–834, 1989.
25. **Wilson, D. F., M. Erecinska, C. Drown, and I. A. Silver.** The oxygen dependence of cellular energy metabolism. *Arch. Biochem. Biophys.* 195: 485–493, 1979.

26. **Wilson, J. R., D. M. Mancini, K. McCully, N. Ferraro, V. Lanoce, and B. Chance.** Noninvasive detection of skeletal muscle underperfusion with near-infrared spectroscopy in patients with heart failure. *Circulation* 80: 1668–1674, 1989.
27. **Wittenberg, B. A., and J. B. Wittenberg.** Transport of oxygen in muscle. *Annu. Rev. Physiol.* 51: 857–878, 1989.
28. **Wittenberg, J. B., and B. A. Wittenberg.** Mechanisms of cytoplasmic hemoglobin and myoglobin function. *Annu. Rev. Biophys. Biophys. Chem.* 19: 217–241, 1990.
29. **Wray, S., M. Cope, D. T. Delpy, J. S. Wyatt, and E. O. R. Reynolds.** Characterization of the near-infrared absorption spectra of cytochrome aa_3 and haemoglobin for the non-invasive monitoring of cerebral oxygenation. *Biochim. Biophys. Acta* 933: 184–192, 1988.
30. **Zijlstra, W. G., A. Buursma, and W. P. Meeuwssen-van der Roest.** Absorption spectra of human fetal and adult oxyhemoglobin, deoxyhemoglobin, carboxyhemoglobin and methemoglobin. *Clin. Chem.* 37: 1633–1638, 1991.

